Global Synthesis of Sea-Surface Temperature Trends During Marine Isotope Stage 11

Yvonne Milker, Rima Rachmayani, Manuel F.G. Weinkauf,
Matthias Prange, Markus Raitzsch, Michael Schulz
and Michal Kučera

Abstract To examine the sea-surface temperature (SST) evolution during interglacial Marine Isotope Stage (MIS) 11, we compiled a database of 78 SST records from 57 sites. We aligned these records by oxygen-isotope stratigraphy and subjected them to an Empirical Orthogonal Function (EOF) analysis. The principal SST trend (EOF1) reflects a rapid deglacial warming of the surface ocean in pace with carbon dioxide rise during Termination V, followed by a broad SST optimum centered at ~410 thousand years (ka) before present (BP). The second EOF indicates the existence of a regional SST trend, characterized by a delayed onset of the SST optimum, followed by a prolonged period of warmer temperatures. The proxy-based SST patterns were compared to CCSM3 climate model runs for three time slices representing different orbital configurations during MIS 11. Although the modeled SST anomalies are characterized by generally lower variance, correlation between modeled and reconstructed SST anomalies suggests a detectable signature of astronomical forcing in MIS 11 climate trends.

Keywords MIS 11 · Interglacial · Quaternary · Sea-surface temperature · Data-model comparison · Empirical orthogonal function

---

Y. Milker (✉) · M.F.G. Weinkauf · M. Kučera
Department of Geosciences, University of Tübingen, Tübingen, Germany
e-mail: Yvonne.Milker@uni-hamburg.de

Y. Milker · R. Rachmayani · M.F.G. Weinkauf · M. Prange · M. Schulz · M. Kučera
MARUM—Center for Marine Environmental Sciences and Faculty of Geosciences,
University of Bremen, Bremen, Germany

M. Raitzsch
Helmholtz Centre for Polar and Marine Research, Alfred Wegener Institute,
Bremerhaven, Germany

Y. Milker
Center for Earth System Research and Sustainability (CEN), Institute for Geology,
University of Hamburg, Hamburg, Germany

M. Schulz and A. Paul (eds.), *Integrated Analysis of Interglacial Climate Dynamics (INTERDYNAMIC)*, SpringerBriefs in Earth System Sciences,
DOI 10.1007/978-3-319-00693-2_3

1 Introduction

Marine Isotope Stage (MIS) 11 (424–374 thousand years (ka) before present (BP)) (Lisiecki and Raymo 2005) was characterized by an unusually long climatic optimum (Tzedakis et al. 2009) with warm conditions lasting longer than in any other mid to late Pleistocene interglacial (Jouzel et al. 2007). The orbital forcing during MIS 11 was characterized by a different phasing of obliquity and precession leading to lower amplitude insolation cycles compared to the Holocene (Loutre and Berger 2003). In contrast to the differences in orbital parameters, the greenhouse gas concentrations in the atmosphere during MIS 11 were similar to the preindustrial Holocene (Siegenthaler et al. 2005). Until now, the coherency of sea-surface temperature (SST) trends during MIS 11 has never been assessed on a global basis. Such comparison is essential for understanding the relationship between SST and climate forcing. In this project, a global compilation of SST records for MIS 11 has been produced, including records covering a large portion of the world ocean on both hemispheres. Our aim was to analyze the roles of orbital and greenhouse gas forcing in MIS 11 climate variability, to detect regional climate variability reflected in SST trends, and to compare the temporal-spatial climate variability simulated by a state-of-the-art climate model for orbital configuration extremes of MIS 11 with that found in proxy records in order to answer the overall question: What are the amplitudes of natural climate variations on timescales of several years to millennia and how do patterns of climate variability vary in time and space?

2 Materials and Methods

We compiled a total of 78 marine SST records from 57 sites (Fig. 1a). We have only used SST records for which also stable oxygen isotope data are available with a sufficient temporal resolution to establish a robust stratigraphic framework. The stratigraphic tuning was carried out against the LR04 stack (Lisiecki and Raymo 2005) [see Milker et al. (2013) for further information]. To extract principal SST modes, the tuned SST records were standardized and interpolated linearly to a temporal resolution of 1,000 years and subjected to an Empirical Orthogonal Function (EOF) analysis. To examine the robustness of the EOF results, we repeated the analysis on randomly resampled age models and SST values with increasing uncertainty. We further performed a resampling approach to test the sensitivity of the EOFs to the number of records used in the analysis. Finally, we compared SST anomalies in the proxy data with climate model outputs for three time slices (394, 405 and 416 ka BP) representing different extremes of the orbital configuration during MIS 11. The time slice simulations were performed with CCSM3, the National Center for Atmospheric Research (NCAR) Community Climate System Model version 3 (see Chap. Comparison of Climate and Carbon Cycle Dynamics During Late Quaternary Interglacials).

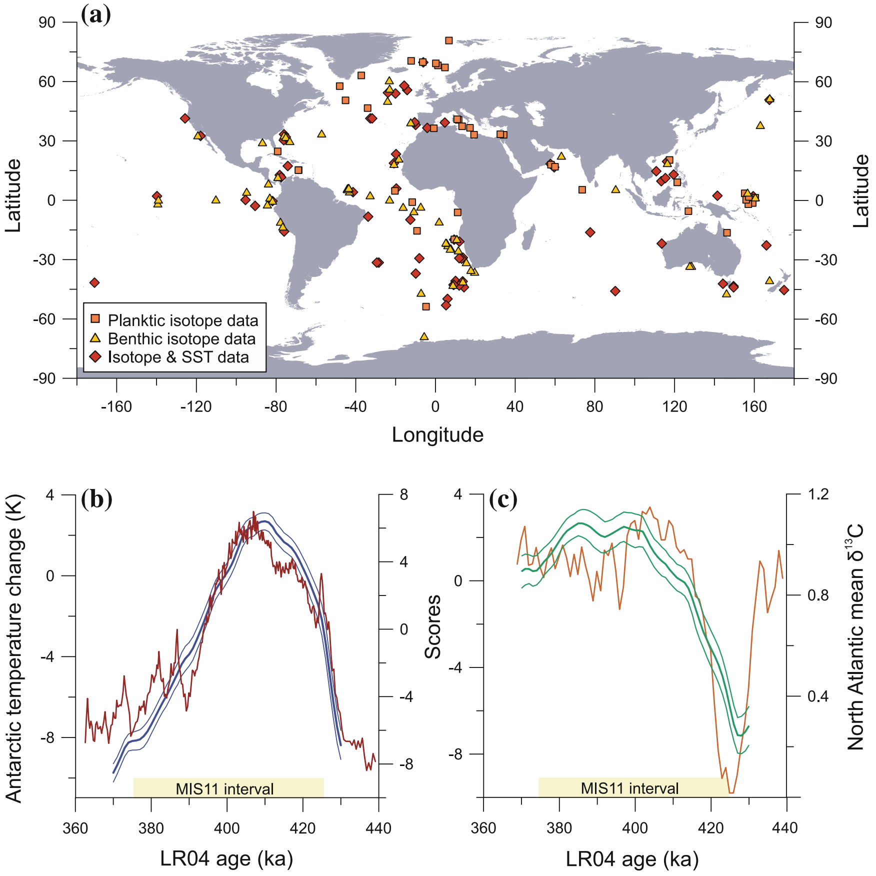

Fig. 1 **a** The location of stable isotope and SST data compiled in the project. **b** Scores of the first EOF with the 95 % confidence interval (age uncertainty set to 5 ka and temperature uncertainty set to 1 °C) compared to the Antarctic temperature change during MIS 11 (Jouzel et al. 2007), **c** Scores of the second EOF with the 95 % confidence interval (age uncertainty set to 5 ka and temperature uncertainty set to 1 °C) compared to deep water mean $\delta^{13}C$ values of the North Atlantic used as a proxy for North Atlantic Deepwater (NADW) production (see also Lisiecki et al. 2008)

3 Key Findings

The EOF analysis reveals two main SST modes (Fig. 1b, c), which explain nearly 70 % of the variation in the dataset, with 49 % explained by EOF1 and ~18 % explained by EOF2. Although we found a stronger influence of temperature uncertainty on the EOF robustness compared to the uncertainty of the age model and reduction of number of records included into analysis, both the shape of the first two EOFs and the amount of variance explained by them are remarkably robust to age-model and temperature uncertainties (Milker et al. 2013).

The first EOF follows a glacial-interglacial pattern with cold SSTs during MIS 12 and MIS 10, and a relatively long duration of warmer SSTs between 416 and 405 ka BP. This trend is similar to the record of Antarctic temperature during MIS 11 (Jouzel et al. 2007), although the interglacial temperature peak is leading the Antarctic record with an offset of ~4 ka (Fig. 1b).This would indicate that during MIS 11, the temperature over Antarctica was not closely coupled to the global mean SST and might have reflected an antiphased southern hemisphere insolation pattern (Laepple et al. 2011). It further seems that the deglacial SST rise, indicated by EOF1 preceded the reduction of the global ice volume (Elderfield et al. 2012) by ~5 ka suggesting a faster reaction of the surface ocean to insolation and greenhouse gas forcing than the response of the slowly melting ice sheets.

The second EOF's scores indicate a later establishment of a relative SST maximum and a longer-lasting period of warmer temperatures during late MIS 11 (Fig. 1c). This regional trend is particularly reflected in the SST records of the mid-latitude North Atlantic Ocean and Mediterranean Sea. The apparently later onset of the MIS 11 optimum and the longer duration of interglacial warmth have also been observed by Voelker et al. (2010), who hypothesized that the associated sustained meltwater input to the (sub-)polar regions may have resulted in a weaker Altantic Meridional Overturning circulation (AMOC). Similarly, mean $\delta^{13}C$ of benthic foraminifera from deeper waters in the North Atlantic used as a proxy for North Atlantic Deepwater (NADW) production (Lisiecki et al. 2008) show a trend of increasing NADW production between 410 and 400 ka BP which is quite similar to the EOF2 scores (Fig. 1c).

The comparison of the proxy-based SST anomalies with CCSM3 model results revealed a large difference in their variance. The range of proxy-based SST anomalies is ~4 °C, whereas modeled SST anomalies vary rarely by more than 1 °C (Milker et al. 2013) (Fig. 2a). The much lower variance in modeled temperature trends might result from an underestimation of temperature changes in climate models, an overestimated proxy SST variability, or from a combination of both. Underestimation of climate variability in model simulations may be caused by shortcomings in the model physics and/or missing climate components resulting in a lack of potentially important feedback mechanisms. Higher variance in the proxy data may result from noise and calibration uncertainties, from larger shifts in the ecology of the microfossils or changes in seasonality and vertical habitats. Despite the large differences in variance and considering all the potential sources of uncertainty in the proxy-based SST values, it is remarkable that in several cases a visual agreement between the direction of proxy and model SST changes emerged (Fig. 2b). Moreover for the boreal summer season of the 416 ka BP time slice as well as for the boreal winter season of the 405 ka BP time slice, a statistically significant correlation between the proxy-based and modeled SST anomalies was found (Milker et al. 2013).This indicates that orbital forcing, the major driver in the CCSM3 experiments, has left a detectable signature in the global SST pattern during MIS 11, despite its unusually low amplitude.

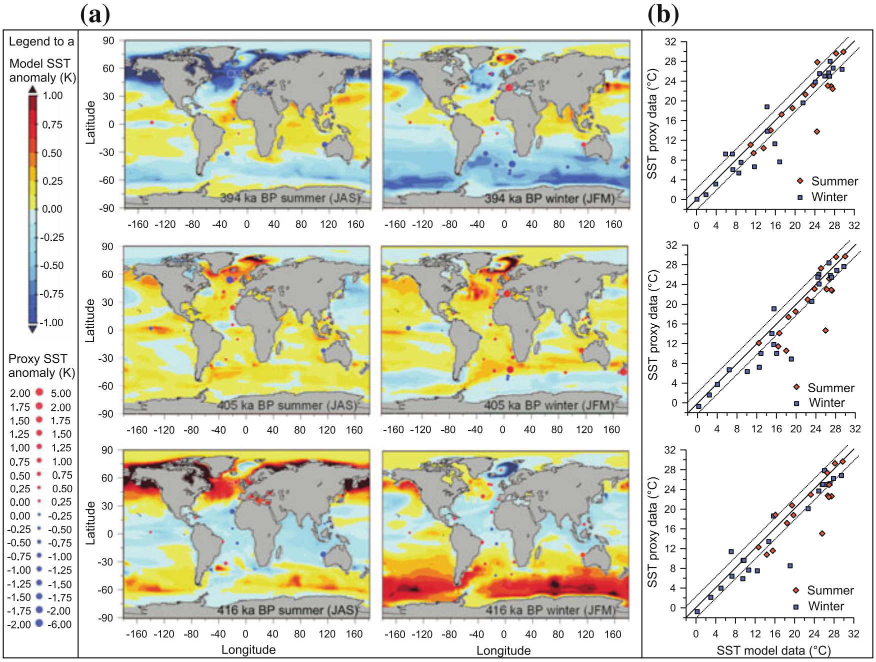

Fig. 2 The distribution of summer and winter SST anomalies modeled by CCSM3 versus proxy-based SST anomalies for the three selected time slices **a** and absolute modeled SST values versus absolute proxy SST values for the same times slices **b**. The *dashed lines* in **b** highlight ±2 °C temperature uncertainty intervals

References

Elderfield H, Ferretti P, Greaves M, Crowhurst S, McCave IN, Hodell D, Piotrowski AM (2012) Evolution of ocean temperature and ice volume through the Mid-Pleistocene climate transition. Science 337:704–709. doi:10.1126/science.1221294

Jouzel J, Masson-Delmotte V, Cattani O, Dreyfus G, Falourd S, Hoffmann G, Minster B, Nouet J, Barnola JM, Chappellaz J, Fischer H, Gallet JC, Johnsen S, Leuenberger M, Loulergue L, Luethi D, Oerter H, Parrenin F, Raisbeck G, Raynaud D, Schilt A, Schwander J, Selmo E, Souchez R, Spahni R, Stauffer B, Steffensen JP, Stenni B, Stocker TF, Tison JL, Werner M, Wolff EW (2007) Orbital and millennial Antarctic climate variability over the past 800,000 years. Science 317:793–796. doi:10.1126/science.1141038

Laepple T, Werner M, Lohmann G (2011) Synchronicity of Antarctic temperatures and local solar insolation on orbital timescales. Nature 471:91–94. doi:10.1038/nature09825

Lisiecki LE, Raymo ME (2005) A Pliocene-Pleistocene stack of 57 globally distributed benthic δ^{18}O records. Paleoceanography 20:PA1003. doi:10.1029/2004PA001071

Lisiecki LE, Raymo ME, Curry WB (2008) Atlantic overturning responses to late Pleistocene climate forcings. Nature 456:85–88. doi:10.1038/nature07425

Loutre MF, Berger A (2003) Marine isotope stage 11 as an analogue for the present interglacial. Global Planet Change 36:209–217. doi:10.1016/S0921-8181(02)00186-8

Milker Y, Rachmayani R, Weinkauf M, Prange M, Raitzsch M, Schulz M, Kučera M (2013) Global and regional sea surface temperature trends during marine isotope stage 11. Clim Past Discuss 9:837–890. doi:10.5194/cpd-9-837-2013

Siegenthaler U, Stocker TF, Monnin E, Lüthi D, Schwander J, Stauffer B, Raynaud D, Bamola JM, Fischer H, Masson-Delmotte V, Jouzel J (2005) Stable carbon cycle-climate relationship during the late Pleistocene. Science 310:1313–1317. doi:10.1126/science.1120130

Tzedakis PC, Raynaud D, McManus JF, Berger A, Brovkin V, Kiefer T (2009) Interglacial diversity. Nat Geosci 2:751–755. doi:10.1038/ngeo660

Voelker AHL, Rodrigues T, Billups K, Oppo D, McManus J, Stein R, Hefter J, Grimalt JO (2010) Variations in mid-latitude North Atlantic surface water properties during the mid-Brunhes (MIS 9–14) and their implications for the thermohaline circulation. Clim Past 6:531–552. doi:10.5194/cp-6-531-2010